Histol Histopathol (2018) 33: 487-495

http://www.hh.um.es

Histology and Histopathology

From Cell Biology to Tissue Engineering

1p36 deletion results in a decrease in glycosaminoglycans which is associated with aggressiveness in neuroblastic tumors

Irene Tadeo[1,2], Esther Gamero-Sandemetrio[1,2], Ana P. Berbegall[1,2], Samuel Navarro[1,2], Adela Cañete[3] and Rosa Noguera[1,2]

[1]Pathology Department, Medical School, University of Valencia-INCLIVA, Valencia, [2]Cancer CIBER (CIBERONC), Madrid and [3]Pediatric Oncology Unit, University and Polytechnic Hospital La Fe, Valencia, Spain

Summary. Despite our deep understanding of neuroblastic tumors, some patients still suffer treatment failure, so pre-treatment risk stratification still requires improvement and the search for new therapeutic targets must continue. Here we correlated prognostic clinical and biological features of neuroblastic tumors with the density of extracellular matrix glycosaminoglycans (the main components of the extracellular matrix 'ground substance'), in nearly 400 primary samples. We also studied the relationship between the density of extracellular matrix glycosaminoglycans and the expression of B3GALT6, an enzyme required for their synthesis. We associated a decrease in glycosaminoglycans with neuroblastomas that were histopathologically poorly-differentiated or undifferentiated, as well as with metastatic disease, and 1p36 deleted tumors. This decrease in glycosaminoglycans was also related to abnormal nuclear B3GALT6 expression in neuroblastic cells. These findings point towards the importance of the ground substance in the aggressiveness of neuroblastic tumors, which should therefore be considered when developing novel therapies for treating neuroblastomas.

Key words: B3GALT6, Glycosaminoglycans, Neuroblastoma, 1p36 deletion, Therapeutic target

Offprint requests to: Professor Rosa Noguera, Pathology Department, Medical School, University of Valencia-INCLIVA, Avda. Blasco Ibáñez, 15, 46010, Valencia, Spain; Cancer CIBER (CIBERONC), Madrid, Spain. e-mail: rnoguera@uv.es

DOI: 10.1467/HH-11-947

Introduction

Glycosaminoglycans (GAGs) constitute the main components of the fundamental or the ground substance of the extracellular matrix (ECM) and can be found as free GAGs or, especially, forming proteoglycans (Noguera et al., 2012). GAGs have unique biofiltering and cell-anchoring properties and are considered to be essential in several biological processes by regulating the main cellular functions (Afratis et al., 2012). Additionally, they have been related to various malignancies and are, therefore, considered to be key players both in cancer cell biology and as novel therapeutic agents (Afratis et al., 2012). The GAG content is affected differently in several malignancies (Bharadwaj et al., 2009; Sironen et al., 2011; Weyers et al., 2012). GAGs usually increase by approximately 15% in aggressive breast cancers compared to non-lethal presentations (Weyers et al., 2012). One particular GAG, hyaluronic acid (HA), accumulates in the stroma of human adenocarcinomas, and other human tumors, and modulates the intracellular signaling pathways, cell

Abbreviations. CS, chondroitin sulfate; dNB, differentiating NB; ECM, extracellular matrix; FISH, fluorescence in situ hybridization; GAGs, glycosaminoglycans; GN, ganglioneuroma; HA, hyaluronic acid; HS, heparan sulfate; iGNB, intermixed ganglioneuroblastoma; INPC, International Neuroblastoma Pathology Classification; INRG, International Neuroblastoma Risk Group; NB, neuroblastoma; NBT, neuroblastic tumors; M, metastatic stage; Ms, metastatic special stage; pdNB, poorly differentiated NB; RGB, red, green, and blue; SNPa, single-nucleotide polymorphism arrays; TMAs, tissue microarrays; uNB, undifferentiated NB

proliferation, motility, and invasive properties of malignant cells (Tammi et al., 2008).

HA is also related to several key biological processes such as host-tumor interactions, vascular and lymphatic angiogenesis, epithelial-mesenchymal transition and, in some adult cancers such as glioma, pancreatic, breast, and prostate cancer, it is related to local and distant metastases (Sironen et al., 2011). Notwithstanding, squamous cell carcinomas and malignant melanomas tend to have a reduced HA content (Bharadwaj et al., 2009). Other studies have found a link between GAG under-sulfation or overexpression of chondroitin sulfate (CS) and poor prognosis in prostate cancer (Ricciardelli et al., 2009; Weyers et al., 2012). GAGs are linked to core proteins and form proteoglycans through a tetrasaccharide linkage region which is synthesized in all secretory cell Golgi complexes (Victor et al., 2009; Vigetti et al., 2014). With the exception of HA, this linkage region is required for GAG biosynthesis, and is catalyzed by four enzymes, which include galactosyltransferase 2, also known as β-3 galactosyltransferase or B3GALT6 (Bai et al., 2001; Hennet, 2002). Of note, defective B3GALT6 has recently been related to skeletal and connective tissue disorders (Malfait et al., 2013; Nakajima et al., 2013; Xu et al., 2014).

Neuroblastic tumors (NBTs) comprise a variety of entities and are a pediatric disease responsible for 15% of childhood deaths from cancer (Kaatsch, 2010). Patients with NBTs present a wide range of clinical evolutions which may result in rapid and aggressive metastatic dissemination or, on the contrary, spontaneous regression (Cohn et al., 2009). Although a recent and well-defined pre-treatment risk classification scheme is now playing a central role in improving survival, more effort must still be made to improve patient survival, both in general and specifically in the high-risk patient subgroup (Pinto et al., 2015).

Recently, Knelson and colleagues (2014) demonstrated that ECM GAGs, especially heparin sulfate (HS), participate in different cellular processes, such as neuroblastic differentiation and cellular progression. Therefore, here we investigated whether the abundance of GAGs was related to prognosis and to metastatic processes in NBT, with the aim of using this as a factor to enhance pre-treatment risk stratification of this disease. We also investigated whether GAGs could be understood as 'cancer attractors' or 'hyperstructures' of therapeutic interest in NBT (Huang et al., 2009). For this purpose, we used digital pathology to quantify GAGs in primary NBT samples, and performed statistical analyses to correlate their density to the International Neuroblastoma Risk Group (INRG) features that have known prognostic value (Cohn et al., 2009) and to other frequent genetic aberrations, in order to determine whether any differences in the ground substance density in NBT and healthy samples are associated with different degrees of malignancy.

Materials and methods

Samples

We analyzed 19 tissue microarrays (TMAs) containing at least two representative 1-mm cylinders taken from 387 primary tumors. All the samples were referred to the Spanish Reference Centre for NBT Biological and Pathological studies (Department of Pathology, University of Valencia-INCLIVA) and had been obtained between 1996 and 2007.

International neuroblastoma risk group biological and clinical data

Paraffin sections were stained with hematoxylin and eosin, underwent immunohistochemistry, and were examined by a pathologist in order to histopathologically categorize NBT following the International Neuroblastoma Pathology Classification (INPC) into: ganglioneuroma (GN), intermixed ganglioneuroblastoma (iGNB), and neuroblastoma (NB) categories, followed by the NB subdivisions: differentiating NB (dNB), poorly-differentiated NB (pdNB), and undifferentiated NB (uNB) (Shimada et al., 1999). GN and iGNB are stroma-rich/stroma-dominant tumors, whereas NBs are stroma-poor tumors; nodular GNBs present mainly stroma-rich areas with nodules of d, pd, and u NB. We considered these tumors to correspond to the NB in the nodular area-the area included in the TMAs. Fluorescence in situ hybridization (FISH) and single-nucleotide polymorphism arrays (SNPa) were performed to assess the genetic changes which the INRG considers to be independent risk factors, such as the status of the MYCN oncogene (amplified or non-amplified) and the 11q23 region (deleted or non-deleted), as well as the presence of the frequently altered 1p36 region (deleted or non-deleted) and 17q chromosome arm (gained or non-gained), following previously published European guidelines (Ambros et al., 2003, 2009; Piqueras et al., 2011; Villamon et al., 2013).

Following the INRG classification scheme, all these variables, along with the stage (localized 1 and 2, metastatic special, and metastatic) and patient age (<18 months or ≥18 months)-information provided by the attending pediatric oncologists or the NBT clinical studies reference center-were used to define the patient risk group (very low, low, intermediate, or high), assign an appropriate probable survival rate, and provide proper treatment (Cohn et al., 2009). The number of samples in each group is shown in Table 1. The different pretreatment risk groups and the 1p36 status, were related to event-free survival as shown in Fig. 1. Patients with high-risk NBT disease and 1p36 deletion had an increased risk of relapse compared to those with lower-risk NBT tumors and an intact 1p36 region.

Histochemistry and immunohistochemistry

For the whole set of samples (from 387 primary tumors), one 3-μm section of each TMA was cut and stained with an Alcian blue pH 2.5 stain kit (Artisan™, Dako) that stains acidic GAGs such as heparan sulfate, dermatan sulfate (HS), CS, and HA, as well as sulfomucins and sialomucins. The density of GAGs was evaluated using image analysis. Immunohistochemistry with anti-B3GALT6 antibody (Abcam ab103375, 1/100), which is physiologically found in the Golgi complex of these cells (Fig. 2), was performed in a subset of 25 samples (18 with 1p36 deletion and 7 with non-deleted 1p36), following the protocol recommended in the datasheet. Expression of the B3GALT6 enzyme by stromal and tumoral cells was assessed and agreed upon by two researchers and was quantified as the percentage of cells of each type expressing the protein in the Golgi complex; we also considered other possible locations for this enzyme.

Image analysis

All TMA slides were scanned with an Aperio XT

Table 1. Clinical and biological variables related with the density of glycosaminoglycans.

Variable	Number of cases	GAG density (median)	Mean ± Standard deviation (minimum-maximum)	Statistical test p-values
Risk group				
High	87	2.10	3.31±4.22 (0.19-32.46)	0.023** (–0.115) (HR vs. IR vs. LR vs. VLR)
Intermediate	29	3.00*	3.97±3.91 (0.31-17.71)	
Low	69	2.85	4.34±4.50 (0.14-20.63)	
Very low	164	3.18	4.07±3.80 (0.37-31.03)	
Stage				
M	89	2.43	3.54±4.28 (0.14-32.46)	0.000** (–0.282) (L1 vs. L2 vs. Ms vs. M) 0.000** (L1+L2 vs. Ms+M)
Ms	26	1.94*	2.83±1.94 (0.49-8.79)	
L2	122	2.58	4.11±4.09 (0.30-20.63)	
L1	130	3.22	4.29±4.13 (0.37-31.03)	
Age				
≥18 months	147	2.90*	4.30±4.82 (0.19-32.46)	0.466
<18 months	223	2.70	3.75±3.55 (0.14-20.36)	
Histopathology (Mean % Schwannian cells)				
uNB (26.92)	44	2.25	3.78±5.14 (0.30-32.46)	0.000** (dNB+pdNB+uNB versus GN+iGNB) 0.007** (–0.153) (dNB vs. pdNB vs. uNB)
pdNB (28.72)	232	2.48	3.45±3.81 (0.14-30.19)	
dNB (32.36)	36	3.24	3.81±2.40 (0.70-11.89)	
iGNB (59.20)	25	4.54	5.72±5.61 (1.28-31.03)	
GN (81.75)	17	6.50	7.83±4.57 (2.49-19.42)	
MYCN				
Amplified	49	2.21	3.23±3.15 (0.30-14.27)	0.060^
Non-Amplified	337	2.88	4.24±4.52 (0.14-32.46)	
11q				
Deleted	61	2.92	3.73±3.52 (0.14-15.78)	0.391
Non-deleted	288	2.84	4.24±4.52 (0.30-32.46)	
1p36~				
Deleted	118	2.43	3.30±3.14 (0.19-19.42)	0.017**
Non-deleted	262	2.93	4.48±4.83(0.14-32.46)	
17q~				
Gained	157	2.71	3.51±3.07 (0.14-17.99)	0.180
Non-gained	202	2.84	4.63±5.27 (0.32-32.46)	

Statistical test p-values: the p-values, coefficient and the variables used for Spearman's rank correlation are indicated in bold font. The rest of the prognostic parameters were analyzed by the Mann-Whitney test; these p-values and variables are also indicated. The categories of the variables are presented from least favorable to most favorable. Abbreviations: GAGs, glycosaminoglycans; VLR, very low risk; LR, low risk; IR, intermediate risk; HR, high risk; M, metastatic; Ms, metastatic special; L, localized; uNB, undifferentiated neuroblastoma; pdNB, poorly differentiated neuroblastoma; dNB, differentiating neuroblastoma; iGNB, intermixed ganglioneuroblastoma; GN, ganglioneuroma; ~denotes frequent genetic changes not considered to define the international NB risk group; ^ denotes that the p-value not statistically significant, but is near the level of significance; ** represent statistically significant differences; * Does not follow the order of decreasing malignancy.

whole-slide scanner (Leica Biosystems, Wetzlar, Germany) at 40× magnification. Each cylinder was analyzed individually with the Aperio Positive Pixel Count Algorithm using Aperio ImageScope software (Leica Biosystems, Wetzlar, Germany). This algorithm counted the number of pixels belonging to a given staining intensity. The intensity of each pixel was the average between the values of red, green, and blue (RGB) intensities. The algorithm was used with the default parameters except for the RGB intensity of the Alcian blue-stained pixels which ranged from 221 to 255. The number of Alcian blue-stained pixels was multiplied by the area of a single pixel (0.25×0.25 μm/pixel, based on the image resolution) to obtain the total Alcian blue-stained area per cylinder. Additionally, the outline of each cylinder was carefully selected in order to measure the area of analysis, and from that, the percentage (%) of Alcian blue-stained area per cylinder; i.e., the GAG density was calculated as the area positive for Alcian blue divided by the total area of the cylinder, multiplied by 100. The density of GAGs per patient sample was calculated using the mean density of the GAGs in all the cylinders from the same patient. Thick fibrous trabeculae were excluded from the analysis. Artefacts, scant material, and lost cylinders were considered as non-evaluable.

Statistical methods

The continuous numerical variable derived from the morphometric analysis did not follow a normal distribution and was therefore correlated to the prognostic INRG categories using the non-parametric Mann-Whitney U test for dichotomized variables and Spearman's rank correlation coefficient for risk, stage, and differentiation-grade variables. A significance level of 95% was established.

Results

Glycosaminoglycans and international neuroblastoma risk group classifications

In general, there were very few GAGs in the ECM of the NBT samples, with a mean density of 4.11±4.37% and a median of 2.82% of the tissue area; the minimum value was 0.14% and the maximum was 32.46% and the median GAG densities and statistical comparisons related to the INRG clinical and biological variables are shown in Table 1. The tumor ECM from patients in the high-risk group usually presented a lower density of GAGs compared to that from non-high risk patients (2.10 vs. 2.75%, respectively). A lower density of GAGs

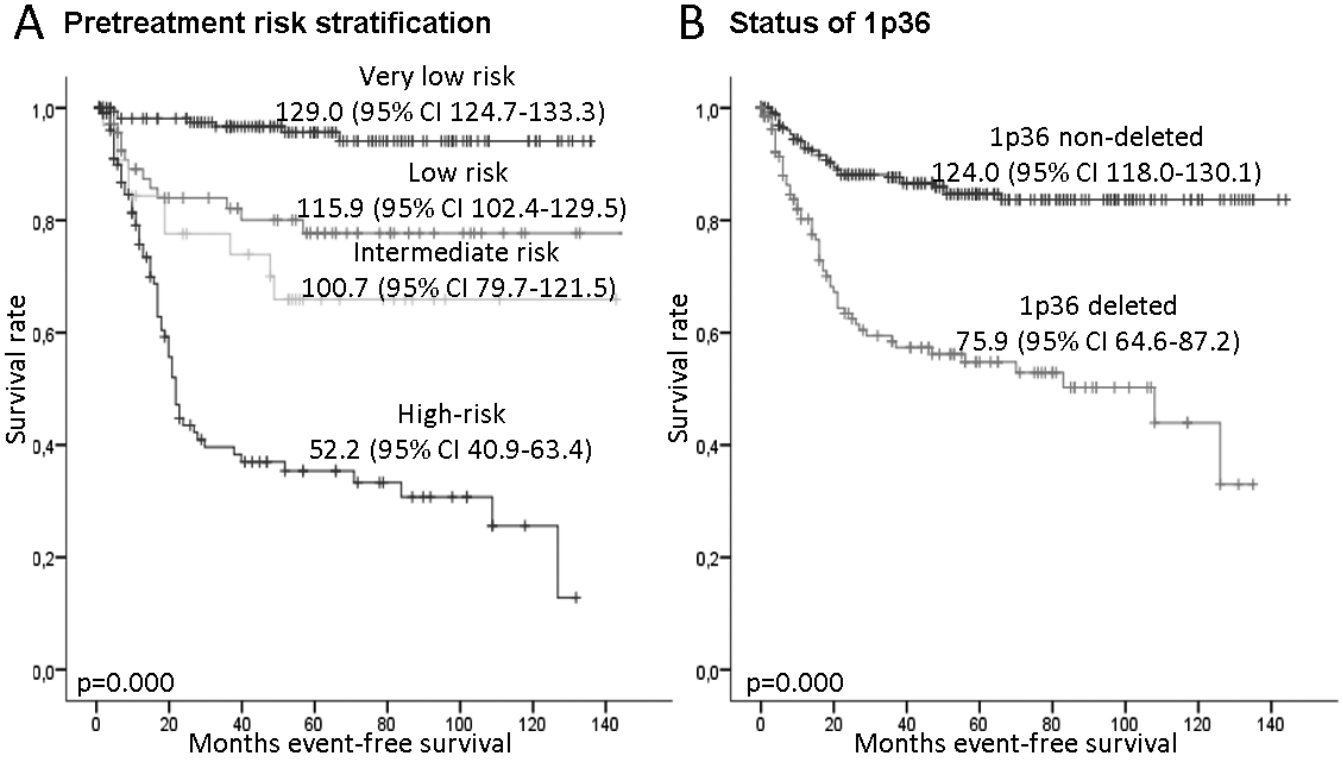

Fig. 1. Kaplan-Meier survival curves with event-free survival in the patients included in the study. **A.** International neuroblastoma risk-group (INRG) pre-treatment stratification. **B.** 1p36 status; the average survival times are shown.

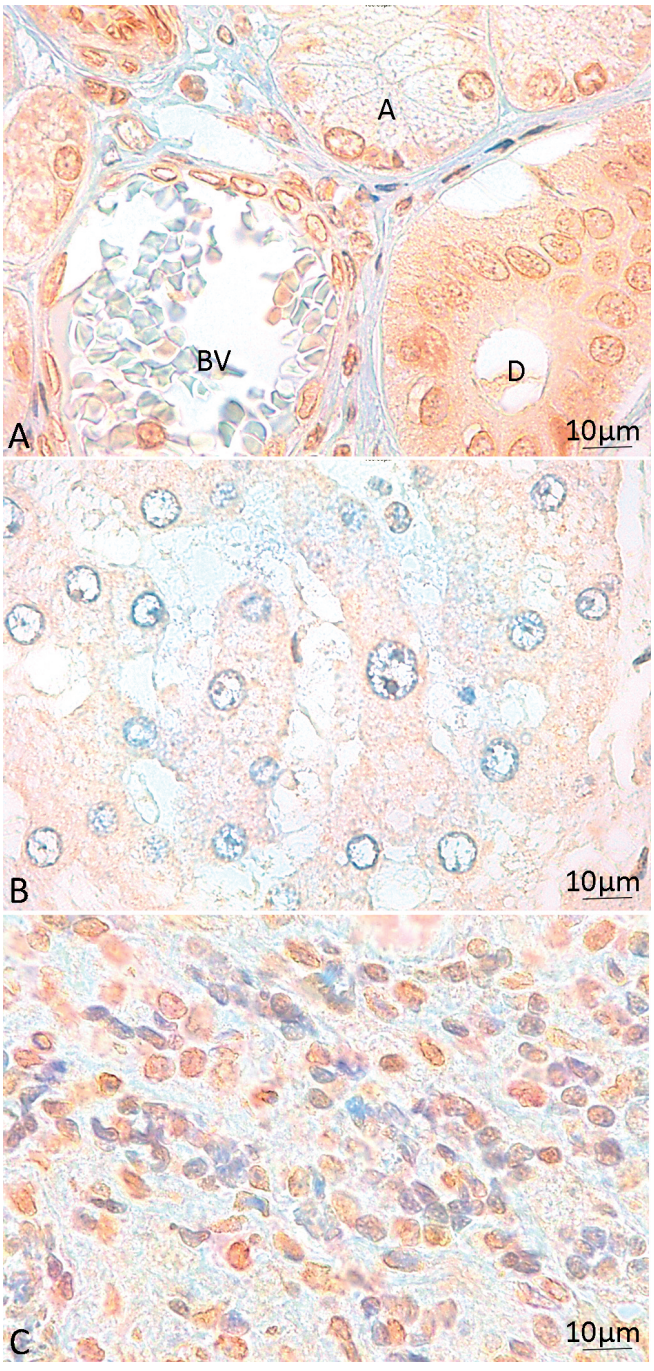

Fig. 2. Expression of the B3GALT6 enzyme in control samples. **A.** Human parotid gland with high perinuclear B3GALT6 expression in the Golgi complex of the cells of acini (A) and ducts (D) as well as positive staining in the endothelial cells of a blood vessel (BV). All these cell types are known for their increased glycosaminoglycan synthesis. **B.** Hepatocytes which are not synthesizing glycosaminoglycans and are neagative for B3GALT6 enzyme staining. **C.** Neuroblastic tumor with intact (non-deleted) 1p, showing perinuclear B3GALT6 expression in the Golgi complexes of stromal and neuroblastic cells (approximately 80% and 60% positive cells, respectively).

was found in NB samples with respect to GN and iGNB samples, and within the NB subset the GAG density was proportionally lower in more undifferentiated NB samples. Both the metastatic stage (M) and the special metastatic stage (Ms), which is related to a better prognosis but greater spreading of the disease compared to the M stage, were associated with the lowest densities of GAGs (2.43% and 1.94%, respectively). The ECM from M or Ms-stage tumors presented significantly fewer GAGs compared with the L1 and L2stages (P=0.000). Finally, the GAG density was significantly lower in samples with 1p36 deletions compared to their non-deleted counterparts (P=0.017). As an illustrative example, the relationship between the histopathology, 1p36 deletion status, and density of GAGs is shown for four cases in Fig. 3.

Glycosaminoglycans and B3GALT6 expression

In the subset of samples that were immunohistochemically studied, B3GALT6 enzyme immunostaining was observed with a perinuclear arrangement in the Golgi complex of Schwann cells in all the samples, in an average 65.2±28.5% cells each (range: 5-95%). Additionally, tumor cells also expressed this enzyme in 80% of the samples, with a mean 12.8±15.4% positive cells each (range: 5-60%). In 46% of the samples, with a mean 27.7±34.5% positive neuroblasts (range: 10-95%), the B3GALT6 enzyme was found in an abnormal subcellular location in the nuclei of tumoral cells. Within the samples with the 1p36 deletion, Golgi complex B3GALT6 enzyme expression was seen in more stromal cells but fewer tumor cells in samples with a low density of GAGs (13 out of 18; 72.2%) compared to samples with higher densities of GAGs (stromal cells: 64.6% vs. 52.0%; tumoral cells: 12.9% vs. 20.0%, respectively). Only the samples with very few GAGs presented nuclear B3GALT6 enzyme accumulation (mean 36.9% of positive neuroblasts). The relationship between the density of GAGs, 1p36 deletion, and B3GALT6 enzyme expression, is explained in Fig. 3 for two cases.

Discussion

In general, we found that the ECM in NBTs contains scant GAGs, which is similar to the stroma of the sympathetic trunk ganglia and the adrenal medulla where these tumors originate. Nevertheless, by analyzing a large cohort of NBT samples by digital pathology, we demonstrated that the low levels of ECM ground substance in these samples is associated with undifferentiated states, metastasis, and 1p36 deletions. In this study, these factors were strongly associated with poor prognosis in NBT patients. Several studies have recently demonstrated the potential of using GAGs as therapeutic targets. For instance, Heymann and colleagues (2016) designed over-sulfated GAGs and found that they inhibited migration and invasiveness *in vitro* in human and murine osteosarcoma cell lines.

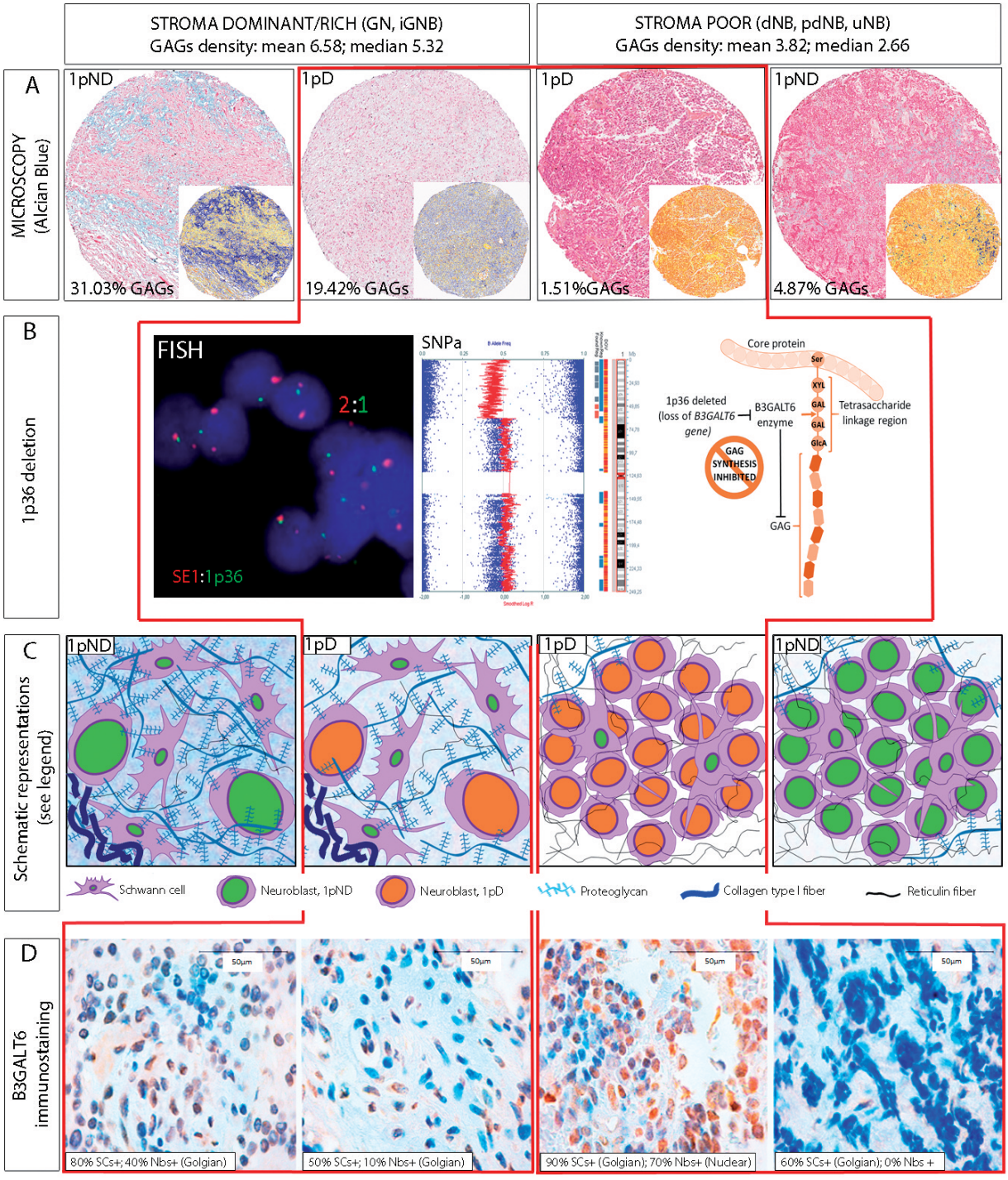

Fig. 3. Relationship between histopathology, glycosaminoglycans (GAGs), 1p36 status, and B3GALT6 enzyme expression in neuroblastic tumors (NBTs). A red line highlights microscopic images and schematic representations of stroma-dominant/rich and stroma-poor NBTs with 1p36 deletion (1pD). **A.** Microscopic images of stroma-dominant/rich and stroma-poor NBTs stained with Alcian blue (GAGs in blue); 1p36 status and GAG densities are indicated. Inserts: mark-up images with GAGs in blue and neuroblastic and stromal cells in orange. **B.** Detection of 1pD and related GAG synthesis. Fluorescence in situ hybridization (FISH; touch preparation), using the chromosome 1 centromere (SE1, in red) and 1p telomere probes (1p36, in green), shows nuclei with 1pD (2:1). Chromosome 1 profile derived from a single nucleotide polymorphism array (SNPa) showing deletion of the 1p arm. Schema representing the hypothetical relationship between 1pD, B3GALT6 gene loss, inhibition of functional B3GALT6 enzyme expression, and a decrease in GAG synthesis. **C.** Schemas of the different NBT histopathologies with 1p36 non-deleted nuclei (1pND, in green) and 1pD nuclei (in orange). In the 1pND samples, cells would be able to synthesize the B3GALT6 enzyme and GAG density would be dependent on the number of Schwann cells, neuroblasts, and other extracellular matrix elements. In the 1pD samples, the stromal cells would mainly be those synthesizing the functional B3GALT6 enzyme, therefore, the GAG density would be higher for the dominant/rich sample and lower for the stroma-poor sample, which will always be lower than their non-deleted counterparts. **D.** Immunostaining of the B3GALT6 enzyme in 1pD samples. Those with a higher density of GAGs (stroma-dominant/rich NBTs) have fewer Schwann cells (SCs+) and more neuroblasts (Nbs+) expressing the B3GALT6 enzyme in the Golgi complex, and show normal B3GALT6 expression in Nbs compared with their stroma-poor NBT counterparts. Only the samples with a lower density of GAGs present abnormal nuclear B3GALT6 enzyme expression.

Thus, we hope that the use of derivative GAG molecules (Pomin, 2015) or the induction of GAG synthesis by restoring the *B3GALT6* gene via nanotechnologies, may be able to inhibit metastatic processes in NB. Therefore, we suggest that GAGs should be considered as targets in NBT.

A low density of glycosaminoglycans is associated with undifferentiated neuroblastoma

Recent studies have demonstrated that ECM GAGs enhance the differentiation of some cell types (Akita et al., 2004) and specifically, HS participates in neuroblastic differentiation, thus suppressing neuroblastoma growth (Knelson et al., 2014). Increased densities of ECM GAGs promotes neuroblastic cell binding to their matrix and, *in vitro*, they settle into this substrate and differentiate (Knelson et al., 2014). In our cohort, the NBT cell differentiation status was inversely related with the density ECM GAGs. In addition, we also found that the quantity of GAGs per tumor sample strongly depended on the abundance of Schwannian stroma (Table 1) which is, in turn, directly related to the INPC NBT histological category-GN, GNB, or NB (Shimada et al., 1999). Furthermore, the NB differentiation grade negatively correlated with GAG density such that low GAG density was associated with lower levels of neuroblastic differentiation (dNB vs. NB vs. uNB, P=0.007).

Low levels of glycosaminoglycans are related to extracellular matrix stiffness and disseminated disease in neuroblastic tumors

HS proteoglycan chains are involved in ECM organization by binding other ECM molecules such as collagens, and their absence promotes invasion and migration in malignant cells (Sanderson, 2001). High ECM HA content is associated with a poor prognosis in breast, lung, and ovarian adenocarcinomas but a good prognosis in squamous cell carcinoma and melanoma (Anttila et al., 2000; Karjalainen et al., 2000; Kosunen et al., 2004); in the latter two, low ECM HA content is also directly correlated with metastatic potential (Karjalainen et al., 2000; Kosunen et al., 2004). Similarly, the overexpression of lumican, another common proteoglycan, favors human colon cancer cell migration by causing filamentous actin reorganization and inhibits melanoma cell migration which is dependent on integrin binding (Radwanska et al., 2012; Pietraszek et al., 2013).

Our group previously described a relationship between fibrous ECM scaffold stiffening and NBT malignancy, whereby abnormal collagen type III or reticulin fiber network organization and increased crosslinking augmented ECM stiffness and porosity (Tadeo et al., 2017), which has been shown to enable tumor cell migration (Seewaldt, 2014). In this current study, the NBT samples with the lowest GAG densities corresponded to metastatic disease stages M and Ms. According to our previous work, the reduced number of GAGs in these tumors favors the occurrence of a rigid ECM scaffolding and, thus, tumor cell migration. Hence, the lower density of GAGs in M-stage tumors in this cohort may have resulted from the increased presence of fibers or cell components in these cells, which would limit the physical space available for GAGs (Tadeo et al., 2017).

The extracellular matrix glycosaminoglycan density is related to neuroblastic cell genetics

To understand the relationship between the 1p36 deletion and the reduced number of GAGs found in our cohort samples, one must understand proteoglycan biosynthesis. A tetrasaccharide linkage region is required for the biosynthesis of all GAGs except for HA, which is catalyzed by three enzymes, including B3GALT6 (Bai et al., 2001; Hennet, 2002). The *B3GALT6* gene is located in the 1p36.33 region and so, abnormal or altered linkage-region synthesis and thereby, also GAG synthesis (except for HA), would be expected if this region is deleted. In line with this, a series of *B3GALT6* mutations was associated with GAG scarcity (Nakajima et al., 2013). Deletions in 1p in NBTs usually include the 1p36.33 region and usually occur in heterozygotes (White et al., 2005; Berbegall et al., 2016). In this study, samples with a low GAG density usually also harbored the 1p36 deletion and presented low B3GALT6 enzyme expression in the Golgi complex as well as abnormal accumulation of this enzyme in the tumoral nuclei. Together, this evidence suggests that the B3GALT6 enzyme produced may not function normally. On the contrary, higher densities of GAGs in samples with the 1p36 deletion may be explained by the presence of varying numbers of Schwann cells where regulated *B3GALT6* enzyme production and GAG synthesis would continue to some degree. In addition, alternative pathways for GAG synthesis, which skip the *B3GALT6* enzymatic polymerization step and could explain this phenomenon, have also been suggested (Nakajima et al., 2013).

Conclusions

Neuroblastic cells with 1p36 deletion and scant ECM GAG underexpress B3GALT6 in the Golgi complex and exhibit abnormal nuclear expression of this enzyme. Consequently, the low density of GAGs in the ECM presumably produced by these changes may contribute to a lack of neuroblastic differentiation and its spread. Thus, because of their strong correlation with some of the variables determining the risk of progression, GAGs and their interacting elements could potentially be used to revert the aggressiveness of NBTs.

Acknowledgements. The authors would like to thank Marcial García Rojo for facilitating the scanning of the samples and Elisa Alonso for technical support. We also want to thank Francisco Santonja and José Bermúdez for support with our statistical analyses. Finally, the authors are grateful to the Spanish Society of Pediatric Hemato-Oncology (SEHOP) for patient data management. This study was supported by FIS contract PI14/01008, RTICC contract RD12/0036/0020, and CIBERONC contract CB16/12/00484, and grants from ISCIII & FEDER (the European Regional Development Fund), Spain. These funding sources played no role in the study design, collection, analysis, or interpretation of the data, or manuscript writing.

References

Afratis N., Gialeli C., Nikitovic D., Tsegenidis T., Karousou E., Theocharis A.D., Pavao M.S., Tzanakakis G.N. and Karamanos N.K. (2012). Glycosaminoglycans: Key players in cancer cell biology and treatment. FEBS J. 279, 1177-1197.

Akita K., Toda M., Hosoki Y., Inoue M., Fushiki S., Oohira A., Okayama M., Yamashina I. and Nakada H. (2004). Heparan sulphate proteoglycans interact with neurocan and promote neurite outgrowth from cerebellar granule cells. Biochem. J. 383, 129-138.

Ambros I.M., Benard J., Boavida M., Bown N., Caron H., Combaret V., Couturier J., Darnfors C., Delattre O., Freeman-Edward J., Gambini C., Gross N., Hattinger C.M., Luegmayr A., Lunec J., Martinsson T., Mazzocco K., Navarro S., Noguera R., O'Neill S., Potschger U., Rumpler S., Speleman F., Tonini G.P., Valent A., Van Roy N., Amann G., De Bernardi B., Kogner P., Ladenstein R., Michon J., Pearson A.D. and Ambros P.F. (2003). Quality assessment of genetic markers used for therapy stratification. J. Clin. Oncol. 21, 2077-2084.

Ambros P.F., Ambros I.M., Brodeur G.M., Haber M., Khan J., Nakagawara A., Schleiermacher G., Speleman F., Spitz R., London W.B., Cohn S.L., Pearson A.D. and Maris J.M. (2009). International consensus for neuroblastoma molecular diagnostics: Report from the international neuroblastoma risk group (inrg) biology committee. Br. J. Cancer 100, 1471-1482.

Anttila M.A., Tammi R.H., Tammi M.I., Syrjanen K.J., Saarikoski S.V. and Kosma V.M. (2000). High levels of stromal hyaluronan predict poor disease outcome in epithelial ovarian cancer. Cancer Res. 60, 150-155.

Bai X., Zhou D., Brown J.R., Crawford B.E., Hennet T. and Esko J.D. (2001). Biosynthesis of the linkage region of glycosaminoglycans: Cloning and activity of galactosyltransferase ii, the sixth member of the beta 1,3-galactosyltransferase family (beta 3galt6). J. Biol. Chem. 276, 48189-48195.

Berbegall A.P., Villamon E., Piqueras M., Tadeo I., Djos A., Ambros P.F., Martinsson T., Ambros I.M., Canete A., Castel V., Navarro S. and Noguera R. (2016). Comparative genetic study of intratumoral heterogenous mycn amplified neuroblastoma versus aggressive genetic profile neuroblastic tumors. Oncogene 35, 1423-1432.

Bharadwaj A.G., Kovar J.L., Loughman E., Elowsky C., Oakley G.G. and Simpson M.A. (2009). Spontaneous metastasis of prostate cancer is promoted by excess hyaluronan synthesis and processing. Am. J. Pathol. 174, 1027-1036.

Cohn S.L., Pearson A.D., London W.B., Monclair T., Ambros P.F., Brodeur G.M., Faldum A., Hero B., Iehara T., Machin D., Mosseri V., Simon T., Garaventa A., Castel V. and Matthay K.K. (2009). The international neuroblastoma risk group (inrg) classification system: An inrg task force report. J. Clin. Oncol. 27, 289-297.

Hennet T. (2002). The galactosyltransferase family. Cell. Mol. Life Sci. CMLS 59, 1081-1095.

Heymann D., Ruiz-Velasco C., Chesneau J., Ratiskol J., Sinquin C. and Colliec-Jouault S. (2016). Anti-metastatic properties of a marine bacterial exopolysaccharide-based derivative designed to mimic glycosaminoglycans. Molecules 21, 309.

Huang S., Ernberg I. and Kauffman S. (2009). Cancer attractors: A systems view of tumors from a gene network dynamics and developmental perspective. Semin. Cell. Dev. Biol. 20, 869-876.

Kaatsch P. (2010). Epidemiology of childhood cancer. Cancer Treat. Rev. 36, 277-285.

Karjalainen J.M., Tammi R.H., Tammi M.I., Eskelinen M.J., Agren U.M., Parkkinen J.J., Alhava E.M. and Kosma V.M. (2000). Reduced level of CD44 and hyaluronan associated with unfavorable prognosis in clinical stage i cutaneous melanoma. Am. J. Pathol. 157, 957-965.

Knelson E.H., Gaviglio A.L., Nee J.C., Starr M.D., Nixon A.B., Marcus S.G. and Blobe G.C. (2014). Stromal heparan sulfate differentiates neuroblasts to suppress neuroblastoma growth. J. Clin. Invest. 124, 3016-3031.

Kosunen A., Ropponen K., Kellokoski J., Pukkila M., Virtaniemi J., Valtonen H., Kumpulainen E., Johansson R., Tammi R., Tammi M., Nuutinen J. and Kosma V.M. (2004). Reduced expression of hyaluronan is a strong indicator of poor survival in oral squamous cell carcinoma. Oral Oncol. 40, 257-263.

Malfait F., Kariminejad A., Van Damme T., Gauche C., Syx D., Merhi-Soussi F., Gulberti S., Symoens S., Vanhauwaert S., Willaert A., Bozorgmehr B., Kariminejad M.H., Ebrahimiadib N., Hausser I., Huysseune A., Fournel-Gigleux S. and De Paepe A. (2013). Defective initiation of glycosaminoglycan synthesis due to b3galt6 mutations causes a pleiotropic ehlers-danlos-syndrome-like connective tissue disorder. Am. J. Hum. Genet. 92, 935-945.

Nakajima M., Mizumoto S., Miyake N., Kogawa R., Iida A., Ito H., Kitoh H., Hirayama A., Mitsubuchi H., Miyazaki O., Kosaki R., Horikawa R., Lai A., Mendoza-Londono R., Dupuis L., Chitayat D., Howard A., Leal G.F., Cavalcanti D., Tsurusaki Y., Saitsu H., Watanabe S., Lausch E., Unger S., Bonafe L., Ohashi H., Superti-Furga A., Matsumoto N., Sugahara K., Nishimura G. and Ikegawa S. (2013). Mutations in b3galt6, which encodes a glycosaminoglycan linker region enzyme, cause a spectrum of skeletal and connective tissue disorders. Am. J. Hum. Genet. 92, 927-934.

Noguera R., Nieto O.A., Tadeo I., Farinas F. and Alvaro T. (2012). Extracellular matrix, biotensegrity and tumor microenvironment. An update and overview. Histol. histopathol. 27, 693-705.

Pietraszek K., Brezillon S., Perreau C., Malicka-Blaszkiewicz M., Maquart F.X. and Wegrowski Y. (2013). Lumican - derived peptides inhibit melanoma cell growth and migration. PloS One 8, e76232.

Pinto N.R., Applebaum M.A., Volchenboum S.L., Matthay K.K., London W.B., Ambros P.F., Nakagawara A., Berthold F., Schleiermacher G., Park J.R., Valteau-Couanet D., Pearson A.D. and Cohn S.L. (2015). Advances in risk classification and treatment strategies for neuroblastoma. J. Clin. Oncol. Off. J. Am. Soc. Clin. Oncol. 33, 3008-3017.

Piqueras M., Subramaniam M.M., Navarro S., Gale N. and Noguera R. (2011). Fluorescence in situ hybridization (FISH) on formalin-fixed paraffin-embedded (FFPE) tissue sections. In: Guidelines for molecular analysis in archive tissues. Stanta G. (ed). Springer.

Trieste, Italy. pp 225-230.

Pomin V.H. (2015). A dilemma in the glycosaminoglycan-based therapy: Synthetic or naturally unique molecules? Med. Res. Rev. 35, 1195-1219.

Radwanska A., Litwin M., Nowak D., Baczynska D., Wegrowski Y., Maquart F.X. and Malicka-Blaszkiewicz M. (2012). Overexpression of lumican affects the migration of human colon cancer cells through up-regulation of gelsolin and filamentous actin reorganization. Exp. Cell Res. 318, 2312-2323.

Ricciardelli C., Sakko A.J., Stahl J., Tilley W.D., Marshall V.R. and Horsfall D.J. (2009). Prostatic chondroitin sulfate is increased in patients with metastatic disease but does not predict survival outcome. Prostate 69, 761-769.

Sanderson R.D. (2001). Heparan sulfate proteoglycans in invasion and metastasis. Semin. Cell. Dev. Biol. 12, 89-98.

Seewaldt V. (2014). ECM stiffness paves the way for tumor cells. Nat. Med. 20, 332-333.

Shimada H., Ambros I.M., Dehner L.P., Hata J., Joshi V.V., Roald B., Stram D.O., Gerbing R.B., Lukens J.N., Matthay K.K. and Castleberry R.P. (1999). The international neuroblastoma pathology classification (the shimada system). Cancer 86, 364-372.

Sironen R.K., Tammi M., Tammi R., Auvinen P.K., Anttila M. and Kosma V.M. (2011). Hyaluronan in human malignancies. Exp. Cell Res. 317, 383-391.

Tadeo I., Berbegall A.P., Navarro S., Castel V. and Noguera R. (2017). A stiff extracellular matrix is associated with malignancy in neuroblastic tumors. Pediatr. Blood Cancer 64, e26449.

Tammi R.H., Kultti A., Kosma V.M., Pirinen R., Auvinen P. and Tammi M.I. (2008). Hyaluronan in human tumors: Pathobiological and prognostic messages from cell-associated and stromal hyaluronan. Semin. Cancer Biol. 18, 288-295.

Victor X.V., Nguyen T.K., Ethirajan M., Tran V.M., Nguyen K.V. and Kuberan B. (2009). Investigating the elusive mechanism of glycosaminoglycan biosynthesis. J. Biol. Chem. 284, 25842-25853.

Vigetti D., Karousou E., Viola M., Deleonibus S., De Luca G. and Passi A. (2014). Hyaluronan: Biosynthesis and signaling. Biochim. Biophys. Acta 1840, 2452-2459.

Villamon E., Berbegall A.P., Piqueras M., Tadeo I., Castel V., Djos A., Martinsson T., Navarro S. and Noguera R. (2013). Genetic instability and intratumoral heterogeneity in neuroblastoma with mycn amplification plus 11q deletion. PloS One 8, e53740.

Weyers A., Yang B., Yoon D.S., Park J.H., Zhang F., Lee K.B. and Linhardt R.J. (2012). A structural analysis of glycosaminoglycans from lethal and nonlethal breast cancer tissues: Toward a novel class of theragnostics for personalized medicine in oncology? OMICS 16, 79-89.

White P.S., Thompson P.M., Gotoh T., Okawa E.R., Igarashi J., Kok M., Winter C., Gregory S.G., Hogarty M.D., Maris J.M. and Brodeur G.M. (2005). Definition and characterization of a region of 1p36.3 consistently deleted in neuroblastoma. Oncogene 24, 2684-2694.

Xu F., Zhang Y.N., Cheng D.H., Tan K., Zhong C.G., Lu G.X., Lin G. and Tan Y.Q. (2014). The first patient with a pure 1p36 microtriplication associated with severe clinical phenotypes. Mol. Cytogenet. 7, 64.

Accepted November 23, 2017